IEEE Access
Multidisciplinary | Rapid Review | Open Access Journal

Received 12 October 2023, accepted 26 October 2023, date of publication 30 October 2023, date of current version 7 November 2023.

Digital Object Identifier 10.1109/ACCESS.2023.3328618

RESEARCH ARTICLE

An Efficient Approach for Recognition of Motor Imagery EEG Signals Using the Fourier Decomposition Method

NEHA SHARMA[1], MANOJ SHARMA[1], (Senior Member, IEEE), AMIT SINGHAL[2], (Senior Member, IEEE), RITESH VYAS[3], (Senior Member, IEEE), HASMAT MALIK[4,5], (Senior Member, IEEE), MOHAMMAD ASEF HOSSAINI[6], AND ASYRAF AFTHANORHAN[7,8]

[1]Electronics and Communication Engineering Department, Bennett University, Greater Noida 201310, India
[2]Electronics and Communication Engineering Department, Netaji Subhas University of Technology, Delhi 110078, India
[3]Department of Information and Communication Technology, Pandit Deendayal Energy University, Gandhinagar, Gujarat 382007, India
[4]Department of Electrical Power Engineering, Faculty of Electrical Engineering, Universiti Teknologi Malaysia, Skudai, Johor Bahru 81310, Malaysia
[5]Department of Electrical Engineering, Graphic Era (Deemed to be University), Dehradun 248002, India
[6]Department of Physics, Badghis University, Badghis 3351, Afghanistan
[7]Faculty of Business and Management, Universiti Sultan Zainal Abidin (UniSZA), Kuala Terengganu, Terengganu 21300, Malaysia
[8]Department of Informatics, Faculty of Social Sciences, Media, and Communication, University of Religions and Denominations, Qom 37100, Iran

Corresponding authors: Hasmat Malik (hasmat.malik@gmail.com), Mohammad Asef Hossaini (asef.hossaini_edu@basu.edu.af), and Asyraf Afthanorhan (asyrafafthanorhan@unisza.edu.my)

This work was supported by the Researchers Supporting Project at Intelligent Prognostic Private Limited Delhi, India, under Project 2023XX2.

ABSTRACT This research paper presents an approach for recognizing motor imagery (MI) movements through brain signals, which has essential applications in assisting people with mobility disorders. One of the critical challenges in this field is that such individuals should be exposed to their surroundings with the help of exact motion recognition. This article represents an algorithm where Fourier-based filters are used for obtaining sub-bands of EEG signals for motion recognition and brain computer interface (BCI) application. Specifically, we segment motor imagery signals into eight orthogonal Fourier intrinsic band functions (FIBFs) and extract statistical feature matrices from each FIBF. We then propose a methodology derived from the k-nearest neighbor (kNN) classifier which is also compared with state-of-the-art classifiers like decision tree (DT), support vector machine (SVM), and naive Bayes (NB), to classify the extracted features and to establish its outperforming nature. Our experimental results show that our proposed approach achieves the highest classification accuracy of 96% and 84.03% with the kNN classifier on the BCI III IVa and BCI IV 2a datasets, outperforming state-of-the-art methods. These results demonstrate the potential of our approach in enabling accurate motion recognition and assisting people with mobility disorders.

INDEX TERMS Electroencephalography, motor imagery, brain–computer interface, k-nearest neighbour, naïve Bayes, decision tree.

I. INTRODUCTION

Brain-computer interface (BCI) development commenced about a century ago when Hans Berger unveiled the brain's electrical activity [1]. BCI is an essential component in the biomedical research community and plays a crucial role in health care. For people who are suffering from spinal cord injury (SCI), paralysis, or any other disorder related to their mobility, BCI helps them in connecting with the external environment. The primary goal of BCI is to use brain-generated electrical signals to control the setting outside the brain [2]. To measure these signals, a non-invasive, portable, low-cost, and high-temporal resolution technique known as electroencephalography (EEG) is employed [3]. Among all the brain signals, sensory-motor rhythms in the brain are responsible for motor-related activities. Motor

The associate editor coordinating the review of this manuscript and approving it for publication was Moussa Ayyash.

imagery (MI) signals are the signals generated while imagining the movement of limbs. MI-EEG is a prevalent experimental paradigm of BCI, and its classification accuracy needs to be improved as it can directly help people suffering from a locked-in state, paralysis, and other mobility-related health problem. The highly accurate and reliable system can be turned into a potential model that can enable disabled people to control external devices, such as prosthetic limbs, wheelchairs, or computers, using only their thoughts. This can improve their independence, communication, and quality of life. The use of MI-EEG-based BCI systems comes with several challenges, like extraction of the desired features to improve classification accuracy, low signal-to-noise ratio (SNR), and a low information transfer rate (ITR) [4]. Other prominent BCI paradigms are steady-state visual evoked potential (SSVEP)-based BCI, P300-based speller, and event-related potential (ERP) [5], [6], [7]. Artefacts contaminate with these signals during recording, and a higher magnitude of any of the artefacts corrupts the EEG signals. These artefacts further complicate the recognition task and can be discarded during preprocessing of the signal [8].

The crucial steps of the standard structure of EEG signal processing are signal acquisition, feature extraction, and classification. Feature selection and algorithm used in signal processing are two essential modules for improving the classification accuracy of MI data. Signal acquisition is the first step for signal processing which may have artefacts contaminated in the signal. Therefore denoising is required for a clean EEG signal. Multi-scale principal component analysis (MSPCA) is an effective technique for denoising an EEG signal [9]. One of the effective feature extractors is the Fourier transform. However, it suffers from the inability to highlight the local spikes and significant sensitivity to noise. These bottlenecks of the Fourier transform encouraged the use of the short-time Fourier transform (STFT), where a window function is introduced to deal with the non-stationary behaviour of EEG signals [10]. However, this technique also has a limitation of confused resolution with narrow and wide window sizes. Wavelet transforms (WT) were also used with different mother wavelets [11]. Here continuous and discrete signals are analyzed with the help of the mother wavelet, scaling factor, and shifting factor that overcomes the disadvantages of STFT. Empirical mode decomposition (EMD) is also used where different intrinsic mode functions (IMFs) are used for the decomposition of the signal [12]. The Fourier decomposition method (FDM) decomposes signal in Fourier intrinsic bands (FIBFS), and each FIBF has a feature vector matrix [13]. Multivariate variational mode decomposition(MVMD) [14] is also used for extracting multi-domain features. Synchro-squeezing wavelet transform (SSWT) [15], Variational mode decomposition [16], and Multivariate Empirical Wavelet Transform (MEWT) [17] are also very popular and robust signal decomposition techniques. Feature optimization and channel selection algorithm was proposed by Jin et al. [18]. Later, the extracted features are passed through various classifiers such as support vector machine (SVM), k-nearest neighbour (kNN), decision tree (DT), and naïve Bayes (NB) to analyze the performance of the signal.

Zhou et al. [19] suggested an STFT-based approach for feature extraction based on the bi-spectrum for the binary class dataset. The authors used conventional second-order features for promising results and suppressed Gaussian noise using the bi-spectrum of the signal. Kervic and Subasi [20] reported analysing binary class motor imagery data using Denoising and segmentation techniques. A set of statistical and higher-order features were used with the kNN classifier. MSPCA was used for denoising, along with different segmentation techniques such as wavelet packet decomposition (WPD), EMD, and DWT. However, selecting the appropriate number of decomposition levels was the limitation of this method. Empirical wavelet transform (EWT) was suggested for signal decomposition for the binary class dataset by Sadiq et al. [21]. Here, selected channels were decomposed into ten adaptive modes analyzed using the Hilbert transform (HT) to obtain instantaneous amplitude and frequency. But there was no explanation of the number of segmented adaptive modes. Singhal et al. [22] used FDM to denoise an electrocardiogram (ECG) signal. The authors removed the ECG signal's power line interference (PLI) and baseline wander (BW). They compared the proposed methodology with normalized sign least mean square (NSLMS), eigenvalue decomposition (EVD), modified recursive least square (MRLS), and EMD-WT. Common spatial pattern (CSP) was also among the MI application's most popular feature extraction techniques. Yongkoo et al. [23], Selim et al. [24], Jin et al. [25] and wang et al. [26] used CSP for the analysis of motor imagery signals. Singh et al. [27] used regularized Riemannian features to analyze EEG signals. Various differential evolution algorithms such as ant colony optimization (ACO) and artificial bee colony (ABC) were proposed by [28] for optimum feature selection. Along with conventional techniques, deep learning-based and transfer-learning approaches are trendy. Dokur et al. [29] proposed a CNN-based classification of the motor-imagery EEG signals. Their proposed CNN was designed to have a reduced number of hyperparameters and yield higher accuracy. Kant et al. [30], and Khedemi et al. [31] proposed CNN-based architectures for recognising motor imagery signals. Researchers also converted EEG time series data into its two-dimensional representation, and further processing was performed. The author [32] utilised phase space dynamics for interpreting EEG data, and then classification is performed based on graphical features. Some recent works [33], [34] presented spatial, temporal, and spectral feature extraction on preprocessed data. One of the most recent approaches for recognizing patterns in EEG data is graphical feature extraction. Authors in [35] used a second-order differential plot (SODP) for extracting graphical features for disease detection. A method for developing subject-dependent and

subject-independent BCI systems is considered in [36] that employs improved empirical Fourier decomposition (IEFD). However, these features must accurately represent the complete information, as some information may get lost in the pre-processing step. Hence, we have trained the models on the raw MI EEG dataset in this paper. Proposed model is based on an effective architecture that achieves good performance for motion recognition, which outperforms the many existing methods [17], [20]. This article proposes feature extraction from raw EEG signals by segmenting them into multiple FIBFs. As each FIBF contributes a feature matrix set, this can result in large feature variability. We then employ various classifiers, including k-nearest neighbour (kNN), decision tree (DT), support vector machine (SVM), and naive Bayes (NB), to classify the extracted features. This results in better recognition of MI movements. Our main contributions are as follows:

- We have considered dyadic cut-off frequencies for decomposing MI-EEG signals since they exhibit significant information at lower frequencies.
- This is the first work considering Fourier-based filters for obtaining sub-bands of EEG signals for BCI application.
- The optimal feature set is derived for extracting information from the sub-bands.
- We conduct an extensive ablation study of MI-EEG signal analysis using various machine learning algorithms, numbers of channels, and FIBFs.
- The proposed framework is more accurate and efficient than existing signal decomposition-based schemes presented in the literature.

The remaining paper is structured as follows: Section II represents the materials and methodology used in the article. This section explains the dataset, methods, extracted features, classifiers, and evaluation metrics implemented in the model. Section III explains the results and discussion of the article. Finally, the article is concluded in section IV.

II. MATERIALS AND METHODOLOGY

In section II, Section II-A provides an analysis of the proposed methodology. Section II-B explains about dataset used for the methodology. All the information on extracted features is discussed in section II-C, whereas subsection II-D provides information on all the classifiers used in the methodology. Finally, evaluation parameters are explained in subsection II-E.

A. FOURIER DECOMPOSITION METHOD

FDM is a signal analysis technique that decomposes a signal into a set of zero mean components called FIBFs with desired cutoff frequencies. The FIBFs are intrinsic in the signal itself and are complete, local, adaptive, and orthogonal [37]. The signal $e\,[m]$ is represented as [13]:

$$e\,[m] = a_0 + \sum_{i=1}^{l} a_i\,[m], \tag{1}$$

where a_0 is the mean value and $a_i[m]$ denote the FIBFs. The block diagram representation of the FDM approach utilizing a zero-phase filter bank [38] based on discrete Fourier transform (DFT) is depicted in Fig.1. The ith filter's frequency response $P_i[n]$ is given by:

$$P_i[n] = \begin{cases} 1 \text{ for } N_{i-1}+1 \le n \le N_i \quad \text{and} \\ L - N_i \le n \le L - N_{i-1} - 1 \\ 0 \text{ otherwise} \end{cases} \tag{2}$$

where $i = 1, 2, \ldots, l$, $N_0 = 0$, $N_l = \frac{L}{2}$ and L is length of the signal. Using inverse DFT (IDFT) operation, the FIBF $a_i\,[m]$ is obtained as:

$$a_i\,[m] = \sum_{n=0}^{L-1} E\,[n]\,P_i\,[n]\,exp\left(\frac{j2\pi nm}{L}\right) \tag{3}$$

with $E\,[n]$ denoting the DFT of the signal, i.e.,

$$E\,[n] = \frac{1}{L}\sum_{m=0}^{L-1} e\,[m]\,exp\left(\frac{-j2\pi nm}{L}\right), 0 \le n \le L-1 \tag{4}$$

The FIBFs $a_i\,[m]$ can be used to build analytic FIBF (AFIBF) representation [13] with instantaneous frequency $w_i\,[m]$ and amplitude $c_i\,[m]$ always greater than zero, i.e., $a_i\,[m] + j\hat{a}_i\,[m] = c_i\,[m]\,exp\,(j\phi_i[m])$ with $c_i\,[m], \omega_i\,[m] \ge 0$, where $\hat{a}_i\,[m]$ denotes the Hilbert transform of $a_i\,[m]$. These AFIBFs are monocomponent signals, and the phase of AFIBF is a monotonically increasing function, such that $w_i\,[m]$ is approximated as:

$$w_i[m] = \left(\frac{\phi_i[m+1] - \phi_i[m-1]}{2}\right) \ge 0 \tag{5}$$

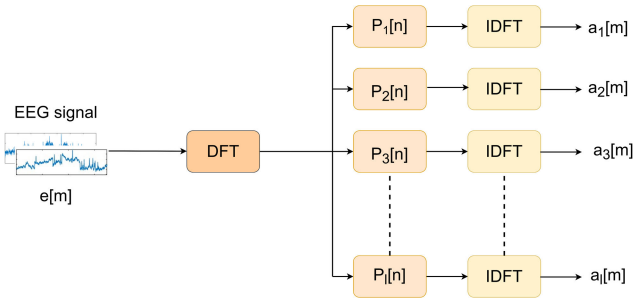

FIGURE 1. Block diagram for FDM based on DFT.

FDM can be implemented using fast Fourier transform (FFT), making it computationally more efficient. It also provides us with a better estimation of time-frequency representation. The TFE representation is beneficial for detecting the dominant components present in the signal [39]. The FIBF represents amplitude and frequency-modulated signals. They correspond to various frequency components present in the signal. With the help of decomposed FIBFs, it becomes easy to identify the desired and useful signal components and separate them from the undesired components of a signal. The FIBFs that correspond to noise can be easily identified and removed simultaneously. Singhal et al. [22] used FDM

to remove BW and PLI from an ECG signal. When we decompose the signal, the first component (0-0.5 Hz) is eliminated as BW. Further, the component around 50 Hz (49.5-50.5 Hz) corresponds to PLI and is also eliminated. The remaining components comprise the clean EEG signal.

The pipeline of the suggested approach is illustrated in Fig.2. The dataset (BCI III IVa) consists of two classes of recorded EEG signals obtained from the imagination of right-foot and right-hand movements. The EEG signal is segmented using FDM into a set of eight orthogonal components (FIBFs), considering uniform frequency bands. A set of statistical and higher-order features are extracted from each FIBF. The obtained feature matrices are passed through various machine learning classifiers such as SVM, kNN, DT, and NB for the classification of foot and right-hand motion recognition. The following subsection describes the suggested approach: the EEG dataset, feature extraction, and a succinct overview of the evaluation metrics attained by motion recognition classifiers.

B. DATASET

A machine running Windows 11 with an Intel(R) Core i5 8265 CPU operating at 1.80 GHz and 8 GB of RAM was used for this investigation. The proposed algorithm was designed and tested in Matlab R2022a.

The BCI competition III dataset IVa is used in this study [40]. This well-known database is accessible to the public and has previously been utilized in several MI-BCI investigations. The data consists of two motor imagery tasks, foot, and right hand. Computer-assisted visual cues from each class were presented to five individuals referred to as ''aa'', ''al'', ''av'', ''aw'', and ''ay'' for 3.5 seconds each. The timing diagram of the applied paradigm is shown in Fig.3. The international 10-20 system was used to record data at 1000 Hz utilizing 118 channels, and later on, the signal was down-sampled at 100 Hz. Therefore, as a result, we acquire a data matrix of 350*118 for each EEG segment of an individual class utilized for every subject. EEG data from five subjects are categorized into training and testing data. Out of 280 recorded trials, 140 belong to the foot, and the other 140 belong to the right hand. The class's original data length is 298458 $\times$ 118, 283574 $\times$ 118, 283042 $\times$ 118,282838 $\times$ 118, and 283562 $\times$ 118, respectively, for both classes of the subjects ''aa,'' ''al,'' ''av,'' ''aw,'' and ''ay''. The labeled number of trials for the right foot and right hand for the ''aa'' subject is 88 and 80, labeled data for both the classes for ''al'' is 112 and for the ''av'' subject is 42, for the ''aw'' subject is 26 and 30, and for the ''ay'' subject is 10 and 18. There are total samples of hand and foot are 98700 and 97300. Out of which we have used 80% of the data for training the models and 20% of the data for testing their performance. We have performed 5-fold cross-validation on this. As we have chosen 20 channels for our analysis.Therefore, as a result, we acquire a data matrix of 98700*20 and 97300*20 for an individual class with segmentation of 350 samples.

The most widely adopted dataset for classifying multiclass MI is BCI IV2a [41], which includes 22 EEG channels and 3 EOG channels. This dataset considered the brain activity of 9 people while they imagined four distinct tasks: left hand (LH), right hand (RH), feet (F), and tongue (T) movements. A total of 288 trials were conducted on all the subjects. The sampling frequency for this dataset is 250 Hz. Though the dataset is recorded for 6 seconds, the motor imagery task is performed between 2-6 seconds. Therefore, as a result, we acquire a data matrix of 1000*22 for each EEG segment of an individual class.

C. FEATURE EXTRACTION

FDM represents signal into a set of FIBFs. However, each FIBF will provide a set of features that are subsequently utilizedÂ for classification. In signals, these features represent important information. As a result, we have utilized these five statistical features in our article.

Mean of signals the absolute value of each FIBF. A bit of information from each observation in a dataset is contained in the mean, which is why it is significant.

$$\mu = \frac{1}{M}\sum_{j=1}^{M}|e_j| \tag{6}$$

Average power of signals in every FIBF. It aids in determining if a survey or experiment result is authentic and noteworthy or just a random outcome.

$$P_e = \sqrt{\frac{1}{L}\sum_{j=1}^{L}e_j^2} \tag{7}$$

Standard deviation of signals in every FIBF. Standard deviation is significant because it helps comprehend measurements when data is diversified.

$$\sigma = \sqrt{\frac{1}{L}\sum_{j=1}^{L}(e_j-\mu)^2} \tag{8}$$

Kurtosis of signals in every FIBF. It is a higher-order statistics feature that describes the spread and height of normal distribution.

$$Ku = \sqrt{\frac{1}{L}\sum_{j=1}^{L}\frac{(e_j-\mu)^4}{\sigma^4}} \tag{9}$$

Skewness of signals in every FIBF. This higher-order statistical feature also describes an asymmetric distribution around the mean.

$$Sk = \sqrt{\frac{1}{L}\sum_{j=1}^{L}\frac{(e_j-\mu)^3}{\sigma^3}} \tag{10}$$

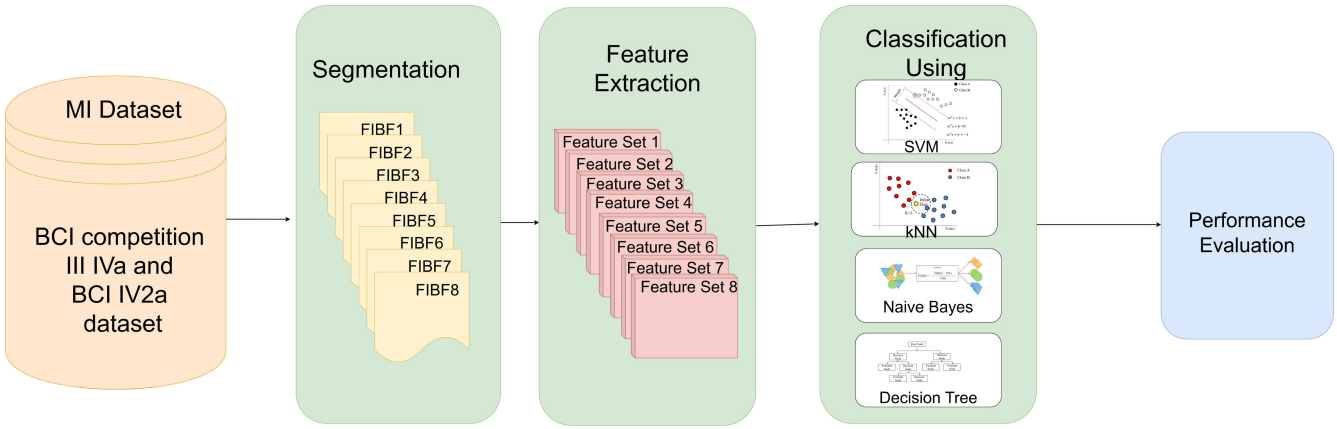

FIGURE 2. Pipeline of the suggested approach.

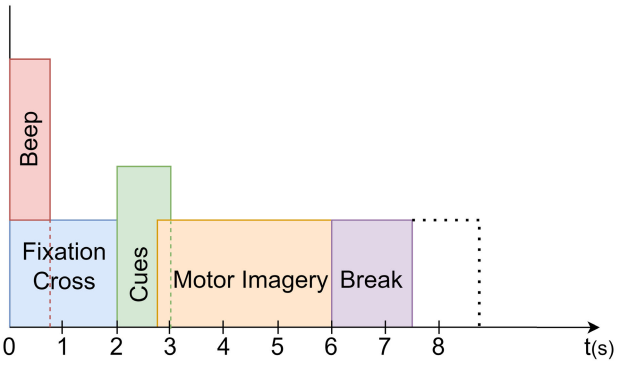

FIGURE 3. Timing of the applied paradigm.

D. CLASSIFICATION

Several classifiers, including SVM, kNN, DT, and NB, are introduced in the subsection to classify motion recognition of the foot and right hand.

1) SUPPORT VECTOR MACHINE (SVM)

SVM is one of the classic algorithms for classifying various data points. Data points, also known as support vectors, are categorized using this method. The kernel function such as radial, polynomial, radial-integral, and linear are used to design a hyperplane for the support vector. A plane that crosses the centre of the data points is known as a hyperplane that produces the correct separation class for the data set. The maximum margin will be in the region enclosed by the hyperplane. The separating hyperplane and the slab's edge are closest to the support vectors of groups $+1$ and -1. Using the appropriate techniques for recognizing support vectors, the margin may be increased to the fullest extent [42]. [43]. Radial basis functions (RBF) kernel was employed in this study.

2) K-NEAREST NEIGHBOUR (KNN)

kNN is a nonlinear classifier employed in the process of classification. This kind of classifier offers reliable performance for the binary class issue and does not require training [44]. Here, the data points are compared with already trained data sets. The data points are classified by the maximum number of nearest neighbours (k). The smaller value of k increases the sensitivity to noise, whereas a larger value increases the computational complexity. First, two-thirds of the entire data are trained, and the final third is tested for the best outcomes. When we need to classify the new data, its distance is measured with neighbours based on the nearness of the data, and the calculated distance is compared with the trained data. Euclidean and Mahalanobis distance metrics are adopted for achieving the best results [45]. Then accordingly, it is labelled in the classes [46].

3) DECISION TREE (DT)

The decision tree is a classification and regression tool. The structure resembles a tree, with each node representing a test performed on the data, each branch for the test's result, and the leaf node for the class label of the data. The top decision node is the root node. There are two basic types of algorithms for constructing a decision tree that is Iterative Dichotomiser 3(ID3) and collection regression tree (CART) [47].

4) NAÏVE BAYES(NB)

A naive Bayes classifier refers to a group of classification techniques centred on the Bayes theorem. Here, every algorithm is predicated on the notion that each pair of classified characteristics is independent of the others. The feature matrix and the response vector are the two critical components of the dataset. Each row in the dataset's feature matrix is a vector, and each vector's value corresponds to a dependent feature's value. Every row of the feature matrix is represented in the response vector by a value for the classification [48].

E. EVALUATION METRICS

System performance can be assessed using a variety of performance metrics, such as accuracy, sensitivity, specificity, etc. A true positive (TP) correctly determines the presence of a condition or characteristic. A false positive (FP) claims

erroneously that a condition or characteristic exists.TN is one that accurately identifies the absence of a condition or trait. FN claims erroneously that a condition or characteristic does not exist [49], [50]. In Fig.4, the confusion matrix for the binary class is depicted.

$$Accuracy = \frac{TP + TN}{TP + TN + FP + FN} \tag{11}$$

$$Senstivity = \frac{TP}{TP + FN} \tag{12}$$

$$Specificity = \frac{TN}{TN + FP} \tag{13}$$

$$Precision = \frac{TP}{TP + FP} \tag{14}$$

$$F - measure = \frac{2TP}{FN + FP + 2TP} \tag{15}$$

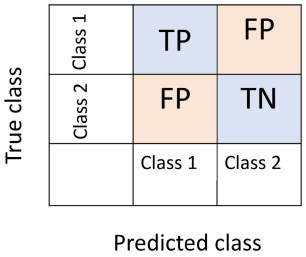

FIGURE 4. Confusion matrix.

III. RESULTS AND DISCUSSION

In this work, all five subjects have different numbers of samples for foot and right-hand motion detection. The FDM method segments whole data into a multiple of 350 samples. We are computing 5 features from every FIBF, giving a total of 40 features considering 8 FIBFs. Further, the dataset is divided into train and test data in the ratio 80:20. The feature selection has not been performed based on performance on the test set. However, the performance on the training set is critical in selecting the optimal features for input to the classifier [20].

Figure 5 demonstrates that the classification accuracy achieved by several classifiers, such as SVM, kNN, decision trees, and naive Bayes, is 88.7%, 96%, 93.1%, and 85.8%, respectively. Therefore, it is evident that with kNN classifier maximum accuracy of 96% is achieved. Fig.5 illustrates that the kNN classifier performs best for 8 FIBFs and 20 channels compared to other classifiers.

The existing works of MI-EEG recognition majorly employ EMD and Wavelet-based approaches, which suffer from respective shortcomings: EMD lacks a rigorous theoretical foundation, whereas the choice of mother wavelet is highly data-dependent. Besides, EMD also suffers from end effects and the mode-mixing problem of IMFs. The proposed approach, devised from FDM and FIBFs, overcomes these limitations and provides a well-justified distinguishing feature vector to attain high classification accuracy. Table 1

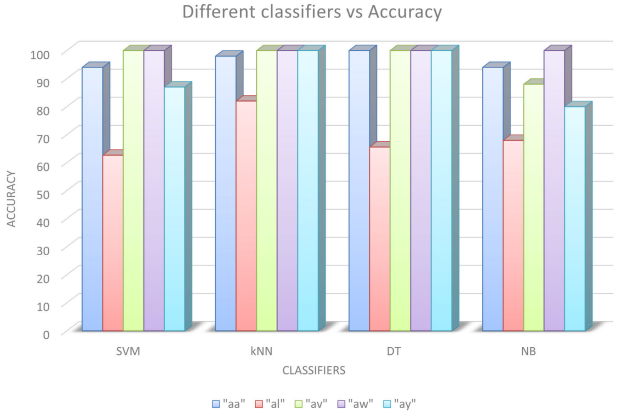

FIGURE 5. A comparative analysis of performance metrics for different classifiers.

illustrates the comparative analysis of these decomposition techniques using the kNN classifier. Wavelet decomposition (WD) technique achieved an average classification accuracy of 82.86% where Daubechies wavelet is used with 3 decomposition levels. An average accuracy of 87.24% was achieved using EMD and FDM achieved the highest classification accuracy of 96% among all the techniques.

TABLE 1. Comparison of different decomposition techniques using kNN classifier.

Decomposition techniques	Accuracy (%)					Avg. acc.(%)
	aa	al	av	aw	ay	
WD	77.3	92.1	53	94.7	97.2	82.86
EMD	86.2	94.2	84.4	77.4	94	87.24
FDM	**98**	**82**	**100**	**100**	**100**	**96**

For BCI applications, tam et al. [51] had suggested that 8-36 channels are adequate to achieve a classification accuracy of 90%. Therefore, we have selected 20 channels from the motor cortex and supplementary motor cortex area based on a 10-20 electrode placement methodology [52]. The performance of the proposed technique depends on the number of FIBFs chosen. Fig 6. shows the performance of the kNN classifier using a different number of FIBFs. We achieved an accuracy of 93.1% for 6 FIBFs, 96% for 8 FIBFs, 84.8% for 10 FIBFs, 95.4% for 12 FIBFs, and 88.8% for 16 FIBFs. The suggested approach provides a maximum accuracy of 96% for 8 FIBFs. Consequently, we used 20 channels and 8 FIBFs.

Table 2 demonstrates the evaluation parameter using a kNN classifier with 8 FIBFs and 20 channels that provide the best average evaluation parameters such as accuracy of 96%, specificity of 95.68%, a sensitivity of 96.36%, a precision of 95.6% and F-1 score of 0.96. Three subjects among five have attained an accuracy of 100%, whereas the other two are above 80%.

Figure 9 illustrates the confusion matrix for each subject. For subject "aa" all the foot samples were correctly identified, whereas only 1 sample of the right hand is wrongly identified as a foot. The accuracy attained by subject "aa"

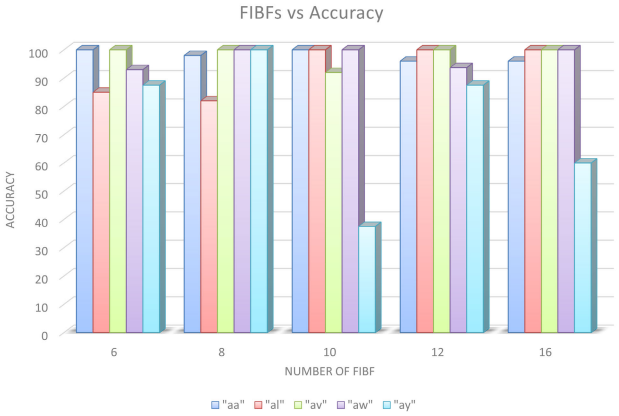

FIGURE 6. Variation in performance with the change in the number of FIBFs.

TABLE 2. Evaluation parameters for all the subjects.

Subject	Accuracy (%)	Specificity (%)	Sensitivity (%)	Precision (%)	F-1 Score
aa	98	96	100	96.2	0.98
al	82	82.4	81.8	81.8	0.82
av	100	100	100	100	1
aw	100	100	100	100	1
ay	100	100	100	100	1

is 98% as shown in Fig.7 (a). In Fig. 7 (b), six samples were wrongly identified for both the classes as the right hand and foot and achieved an accuracy of 82%. For subjects ''av'', ''aw'', and ''ay'', an accuracy of 100% is achieved as demonstrated in Fig. 7 (c), 7 (d), 7 (e).

The multiclass dataset's confusion matrix is depicted in Fig.8. Out of a total of 170 samples, 138 samples of LH were accurately classified as LH, which constitutes 20% of the entire LH dataset. On the other hand, there were 15 instances of RH misclassified, 12 samples of F incorrectly classified, and 5 samples of T misclassified. The proposed methodology accurately identified 142 samples of RH, 135 samples of F, and 164 samples of T out of 173 samples of each class. Table 3 displays the performance measures computed from the confusion matrix whereas the classification accuracy for individual subject is shown in table 4.

For a limited sample set, Kervic et al. implemented MSPCA with WPD and classified it using kNN [20]. Here, the authors have ablated a set of features and achieved an accuracy of 92.8%. Sadiq et al. [21] proposed EWT for 18 channels only and achieved an accuracy of 95.2%. Yongkoo et al. [23], suggested an approach where locally generated CSP features centered at each channel are extracted from EEG data, and with these features, an accuracy of 84.4% is achieved. Selim et al. [24] discussed CSP on nine bands over a selected time interval. Later, extracted features are passed through optimized SVM and achieved an accuracy of 85.01%. For a fair comparison, the proposed approach by Dokur and Olmez [29] is only compared against the results of the no transformation stage (NTS) and non-augmented (NA). The authors achieved a classification accuracy of 73.4%, whereas the proposed approach yields a classification accuracy of 98.5%. Belwafi et al. [53] proposed dynamic filtering using the weight overlap-add (WOLA) algorithm. Then, based on spatial features EEG signal is classified using LDA. An enhanced version of LDA is proposed by Zhang et al. [54]. In this, the decision boundary is decided by z-score using mean and std. deviation. The proposed decision boundary definition strategy attains an accuracy of 81.1%. Dai et al. [55] suggested an approach with transfer kernel CSP.

The authors improved the model's performance by the learning domain-independent kernel and obtained a classification accuracy of 81.14%. Jin et al. [56], Rashid et al. [57], and Murguia et al. [58] extracted features using CSP and achieved an accuracy of 87.3%, 93.6%, and 74.9% respectively. Sadiq et al. [59] suggested 2-D modelling using EWT and attained a classification accuracy of 95.3%. Table 2 shows the classification accuracy of the proposed methodology along with other methodologies. Therefore, the proposed methodology achieves the highest accuracy among all the other methodologies. Out of five subjects, three subjects achieved 100% accuracy.

TABLE 3. Performance evaluation of multiclass dataset for each class.

Class	Accuracy (%)	Specificity (%)	Sensitivity (%)	Precision (%)	F-1 Score
LH	90.86	94	82	81	0.81
RH	92.1	95.5	86	82	0.84
F	91	95.3	85	78	.81
T	94.05	93.7	84	95	.89

TABLE 4. Classification accuracy obtained for individual subjects.

Subject	A01	A02	A03	A04	A05	A06	A07	A08	A09
Acc.(%)	79.7	70.2	82.1	84.5	88	84.7	91.6	83.3	84.5

Sakhavi et al. [60] proposed a three-layer CNN model to classify filter bank common spatial pattern (FBCSP) features and attained an accuracy of 74%. Xu et al. [65] suggested narrow FBCSP (NFBCSP) technique for optimum features and attained a classification accuracy of 76.8%. Lu et al. [61] suggested a hybrid approach with CNN and LSTM and achieved a classification accuracy of 76.6%. A bidirectional GRU network was proposed by Qiao and Bi et al. [62] and obtained a classification accuracy of 76.62%. Riyad et al. [63] proposed a pre trained EEGnet with which the author achieved an accuracy of 74%. Liao et al. [64] converted EEG data into an image and used 2D representation with shallow CNN to achieve a classification accuracy of 74.6%. Our results are on par with state-of-the-art methods that employ deep learning on MI recognition tasks by converting the 1-dimensional (1D) data into 2-dimensional (2D) images. Our proposed method offers the advantage of

FIGURE 7. Confusion matrix using kNN classifier for (a) "aa" subject (b) "al" subject (c) "av" subject (d) "aw" subject (e) "ay" subject.

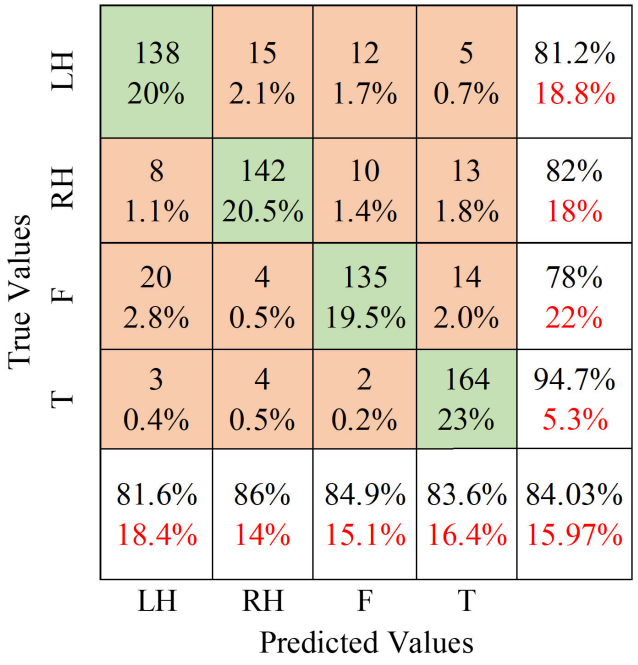

FIGURE 8. Confusion matrix using kNN classifier for multiclass dataset.

TABLE 5. Comparison of proposed techniques with state-of-the-art techniques for binary class dataset.

Author	Methodology	Accuracy (%)					Avg. acc.(%)
		aa	al	av	aw	ay	
Kervic et al. [20]	WPD	96	92.3	88.9	95.4	91.4	92.8
Sadiq et al. [21]	EWT	94.5	91.7	97.2	95.6	97	95.2
Yongkoo et al. [23]	CSP feature	100	74.1	67.8	90	89.2	84.4
Selim et al. [24]	CSP\AM-BA	86.6	100	66.8	96.3	80.9	85.01
Dokur et al. [29]	CNN(NTS-NA)	85.4	60	65.4	83.6	72.7	73.4
Belwafi et al. [53]	Adaptive filter bank	66.8	96.1	52.1	71.4	50	67.3
Zhang et al. [54]	Z-LDA	77.7	100	68.4	99.6	59.9	81.1
Dai et al. [55]	CSP	68.1	93.9	68.5	90.5	84.7	81.4
Jin et al. [56]	CSP	82.1	93.9	73.6	93.6	93.2	87.3
Rashid et al. [57]	CSP	94.6	94.6	95	93.2	90.1	93.6
Murguia et al. [58]	CSP	73.2	83.9	64.8	75	77.4	74.9
Sadiq et al. [59]	EWT	99.4	98.7	92.2	85.7	100	95.3
Proposed methodology		98	82	100	100	100	96

reduced computational complexity by directly applying FDM methodology on the raw EEG data (1D data). This makes our approach more efficient. The comparison is shown in table 6. It is worth specifying here that the proposed approach achieves the binary classification accuracy of 96% without any preprocessing techniques, which is contrary to various related works. Concurrently, the model achieves comparable accuracy of 84.03% for the multiclass classification problem, which asserts its effectiveness in a generalized scenario since

TABLE 6. Comparison of proposed techniques with state-of-the-art techniques for multiclass dataset.

Author	Methodology	Input Formulation	Accuracy (%)
Sakhavi et al. [60]	CNN+FBCSP	Time-series EEG signal	74
Lu et al. [61]	CNN+LSTM	Time-series EEG signal	76.6
Qiao and Bi et al. [62]	GRU	Time-series EEG signal	76.6
Riyad et al. [63]	EEGnet	Time-series EEG signal	74
Liao et al. [64]	Shallow CNN	EEG as image(2D)	74.6
Xu et al. [65]	NFBCSP	Time-series EEG signal	76.8
Proposed Methodology		Time-series EEG signal	84.03

the proposed approach is validated on two different datasets of different sampling frequencies.

IV. CONCLUSION

This article proposes a method for motion recognition of the left hand, right hand, foot, and tongue from MI EEG data. In the proposed method, segmentation of EEG data is performed using FDM and is classified using a machine learning classifier. The results reveal that with this publically available dataset, left-hand, right-hand foot, and tongue motions are correctly recognized using FDM. In the study, FDM segments the data, and extracted features from segmented data are fed to various machine learning classifiers such as SVM, kNN, DT, and NB. With an accuracy of 96% for binary and 84.03% for multiclass, kNN classifier outperforms all others in terms of performance.

Our future research endeavors will focus on collecting a diverse dataset and leveraging advanced training techniques to improve the generalization capabilities of our machine learning models. We will also explore the use of deep features using 1-Dimensional CNN along with FDM-based features and their fusion at different levels to get better performance. This diverse dataset will be used to train our models, enhancing their ability to generalize across various applications. The goal is to develop models that can adapt and perform reliably in real-world scenarios, ensuring their practical utility and robustness.

REFERENCES

[1] H. Altaheri, G. Muhammad, M. Alsulaiman, S. U. Amin, G. A. Altuwaijri, W. Abdul, M. A. Bencherif, and M. Faisal, "Deep learning techniques for classification of electroencephalogram (EEG) motor imagery (MI) signals: A review," *Neural Comput. Appl.*, pp. 1–42, Aug. 2021.

[2] S. Abenna, M. Nahid, and A. Bajit, "Motor imagery based brain-computer interface: Improving the EEG classification using delta rhythm and LightGBM algorithm," *Biomed. Signal Process. Control*, vol. 71, Jan. 2022, Art. no. 103102.

[3] N. Sharma, M. Sharma, A. Singhal, R. Vyas, H. Malik, A. Afthanorhan, and M. A. Hossaini, "Recent trends in EEG-based motor imagery signal analysis and recognition: A comprehensive review," *IEEE Access*, vol. 11, pp. 80518–80542, 2023.

[4] N. Padfield, J. Zabalza, H. Zhao, V. Masero, and J. Ren, "EEG-based brain–computer interfaces using motor-imagery: Techniques and challenges Natasha," *Sensors*, vol. 19, no. 1423, pp. 1–34, 2019.

[5] J. Jin, Z. Wang, R. Xu, C. Liu, X. Wang, and A. Cichocki, "Robust similarity measurement based on a novel time filter for SSVEPs detection," *IEEE Trans. Neural Netw. Learn. Syst.*, vol. 34, no. 8, pp. 4096–4105, Aug. 2023.

[6] M. Xu, J. Han, Y. Wang, T.-P. Jung, and D. Ming, "Implementing over 100 command codes for a high-speed hybrid brain–computer interface using concurrent P300 and SSVEP features," *IEEE Trans. Biomed. Eng.*, vol. 67, no. 11, pp. 3073–3082, Nov. 2020.

[7] J. Pan, Q. Xie, P. Qin, Y. Chen, Y. He, H. Huang, F. Wang, X. Ni, A. Cichocki, R. Yu, and Y. Li, "Prognosis for patients with cognitive motor dissociation identified by brain–computer interface," *Brain*, vol. 143, no. 4, pp. 1177–1189, Apr. 2020.

[8] X. Jiang, G.-B. Bian, and Z. Tian, "Removal of artifacts from EEG signals: A review," *Sensors*, vol. 19, no. 5, p. 987, Feb. 2019.

[9] M. T. Sadiq, X. Yu, Z. Yuan, M. Z. Aziz, S. Siuly, and W. Ding, "Toward the development of versatile brain–computer interfaces," *IEEE Trans. Artif. Intell.*, vol. 2, no. 4, pp. 314–328, Aug. 2021.

[10] G. Xu, X. Shen, S. Chen, Y. Zong, C. Zhang, H. Yue, M. Liu, F. Chen, and W. Che, "A deep transfer convolutional neural network framework for EEG signal classification," *IEEE Access*, vol. 7, pp. 112767–112776, 2019.

[11] E. Hernández-González, P. Gómez-Gil, E. Bojorges-Valdez, and M. Ramírez-Cortés, "Bi-dimensional representation of EEGs for BCI classification using CNN architectures," in *Proc. 43rd Annu. Int. Conf. IEEE Eng. Med. Biol. Soc. (EMBC)*, Nov. 2021, pp. 767–770.

[12] U. Maji and S. Pal, "Empirical mode decomposition vs. variational mode decomposition on ECG signal processing: A comparative study," in *Proc. Int. Conf. Adv. Comput., Commun. Informat. (ICACCI)*, Sep. 2016, pp. 1129–1134.

[13] P. Singh, S. D. Joshi, R. Kumar, and K. Saha, "The Fourier decomposition method for nonlinear and non-stationary time series analysis," *Proc. Roy. Soc. A, Math., Phys. Eng. Sci.*, vol. 473, no. 2199, p. 0871, Mar. 2017.

[14] M. T. Sadiq, X. Yu, Z. Yuan, M. Z. Aziz, N. U. Rehman, W. Ding, and G. Xiao, "Motor imagery BCI classification based on multivariate variational mode decomposition," *IEEE Trans. Emerg. Topics Comput. Intell.*, vol. 6, no. 5, pp. 1177–1189, Oct. 2022.

[15] S. Mamli and H. Kalbkhani, "Gray-level co-occurrence matrix of Fourier synchro-squeezed transform for epileptic seizure detection," *Biocybernetics Biomed. Eng.*, vol. 39, no. 1, pp. 87–99, Jan. 2019.

[16] M. K. Islam Molla, S. Das, M. E. Hamid, and K. Hirose, "Empirical mode decomposition for advanced speech signal processing," *J. Signal Process.*, vol. 17, no. 6, pp. 215–229, 2013.

[17] M. T. Sadiq, X. Yu, Z. Yuan, F. Zeming, A. U. Rehman, I. Ullah, G. Li, and G. Xiao, "Motor imagery EEG signals decoding by multivariate empirical wavelet transform-based framework for robust brain–computer interfaces," *IEEE Access*, vol. 7, pp. 171431–171451, 2019.

[18] J. Jin, Y. Miao, I. Daly, C. Zuo, D. Hu, and A. Cichocki, "Correlation-based channel selection and regularized feature optimization for MI-based BCI," *Neural Netw.*, vol. 118, pp. 262–270, Oct. 2019.

[19] S.-M. Zhou, J. Q. Gan, and F. Sepulveda, "Classifying mental tasks based on features of higher-order statistics from EEG signals in brain–computer interface," *Inf. Sci.*, vol. 178, no. 6, pp. 1629–1640, Mar. 2008.

[20] J. Kevric and A. Subasi, "Comparison of signal decomposition methods in classification of EEG signals for motor-imagery BCI system," *Biomed. Signal Process. Control*, vol. 31, pp. 398–406, Jan. 2017.

[21] M. T. Sadiq, X. Yu, Z. Yuan, Z. Fan, A. U. Rehman, G. Li, and G. Xiao, "Motor imagery EEG signals classification based on mode amplitude and frequency components using empirical wavelet transform," *IEEE Access*, vol. 7, pp. 127678–127692, 2019.

[22] A. Singhal, P. Singh, B. Fatimah, and R. B. Pachori, "An efficient removal of power-line interference and baseline wander from ECG signals by employing Fourier decomposition technique," *Biomed. Signal Process. Control*, vol. 57, Mar. 2020, Art. no. 101741.

[23] Y. Park and W. Chung, "BCI classification using locally generated CSP features," in *Proc. 6th Int. Conf. Brain-Computer Interface (BCI)*, Jan. 2018, pp. 1–4.

[24] S. Selim, M. M. Tantawi, H. A. Shedeed, and A. Badr, "A CSP\AM-BA-SVM approach for motor imagery BCI system," *IEEE Access*, vol. 6, pp. 49192–49208, 2018.

[25] J. Jin, R. Xiao, I. Daly, Y. Miao, X. Wang, and A. Cichocki, "Internal feature selection method of CSP based on L1-norm and Dempster–Shafer theory," *IEEE Trans. Neural Netw. Learn. Syst.*, vol. 32, no. 11, pp. 4814–4825, Nov. 2021.

[26] J. Wang, Z. Feng, N. Lu, L. Sun, and J. Luo, "An information fusion scheme based common spatial pattern method for classification of motor imagery tasks," *Biomed. Signal Process. Control*, vol. 46, pp. 10–17, Sep. 2018.

[27] A. Singh, S. Lal, and H. W. Guesgen, "Small sample motor imagery classification using regularized Riemannian features," *IEEE Access*, vol. 7, pp. 46858–46869, 2019.

[28] M. Z. Baig, N. Aslam, H. P. H. Shum, and L. Zhang, "Differential evolution algorithm as a tool for optimal feature subset selection in motor imagery EEG," *Exp. Syst. Appl.*, vol. 90, pp. 184–195, Dec. 2017.

[29] Z. Dokur and T. Olmez, "Classification of motor imagery electroencephalogram signals by using a divergence based convolutional neural network," *Appl. Soft Comput.*, vol. 113, Dec. 2021, Art. no. 107881.

[30] P. Kant, S. H. Laskar, J. Hazarika, and R. Mahamune, "CWT based transfer learning for motor imagery classification for brain computer interfaces," *J. Neurosci. Methods*, vol. 345, Nov. 2020, Art. no. 108886.

[31] Z. Khademi, F. Ebrahimi, and H. M. Kordy, "A transfer learning-based CNN and LSTM hybrid deep learning model to classify motor imagery EEG signals," *Comput. Biol. Med.*, vol. 143, Apr. 2022, Art. no. 105288.

[32] M. T. Sadiq, H. Akbari, S. Siuly, Y. Li, and P. Wen, "Alcoholic EEG signals recognition based on phase space dynamic and geometrical features," *Chaos, Solitons Fractals*, vol. 158, May 2022, Art. no. 112036.

[33] Y. Song, X. Jia, L. Yang, and L. Xie, "Transformer-based spatial–temporal feature learning for EEG decoding," 2021, *arXiv:2106.11170*.

[34] Y. Ma, Y. Song, and F. Gao, "A novel hybrid CNN-transformer model for EEG motor imagery classification," in *Proc. Int. Joint Conf. Neural Netw. (IJCNN)*, 2022, pp. 1–8.

[35] H. Akbari, M. T. Sadiq, N. Jafari, J. Too, N. Mikaeilvand, A. Cicone, and S. Serra-Capizzano, "Recognizing seizure using Poincaré plot of EEG signals and graphical features in DWT domain," *Bratislava Med. J.*, vol. 124, no. 1, pp. 12–24, 2022.

[36] X. Yu, M. Z. Aziz, M. T. Sadiq, Z. Fan, and G. Xiao, "A new framework for automatic detection of motor and mental imagery EEG signals for robust BCI systems," *IEEE Trans. Instrum. Meas.*, vol. 70, pp. 1–12, 2021.

[37] N. Sharma, M. Sharma, and A. Singhal, "Feature extraction for motor imagery signals using the Fourier decomposition method to boost recognition performance," in *Proc. 5th Biennial Int. Conf. Innov. Appl. Comput. Intell. Power Energy Control Impact Humanity*, 2022, p. 40.

[38] B. Fatimah, P. Singh, A. Singhal, and R. B. Pachori, "Detection of apnea events from ECG segments using Fourier decomposition method," *Biomed. Signal Process. Control*, vol. 61, Aug. 2020, Art. no. 102005.

[39] P. Singh, A. Singhal, and S. D. Joshi, "Time-frequency analysis of gravitational waves," in *Proc. Int. Conf. Signal Process. Commun. (SPCOM)*, Jul. 2018, pp. 197–201.

[40] B. Blankertz, K.-R. Müller, D. J. Krusienski, G. Schalk, J. R. Wolpaw, A. Schlogl, G. Pfurtscheller, J. R. Millan, M. Schroder, and N. Birbaumer, "The BCI competition III: Validating alternative approaches to actual BCI problems," *IEEE Trans. Neural Syst. Rehabil. Eng.*, vol. 14, no. 2, pp. 153–159, Jun. 2006.

[41] M. Tangermann, K.-R. Müller, A. Aertsen, N. Birbaumer, C. Braun, C. Brunner, R. Leeb, C. Mehring, K. J. Miller, G. R. Müller-Putz, G. Nolte, G. Pfurtscheller, H. Preissl, G. Schalk, A. Schlögl, C. Vidaurre, S. Waldert, and B. Blankertz, "Review of the BCI competition IV," *Frontiers Neurosci.*, vol. 6, pp. 6–55, Jul. 2012.

[42] D. Garrett, D. A. Peterson, C. W. Anderson, and M. H. Thaut, "Comparison of linear, nonlinear, and feature selection methods for EEG signal classification," *IEEE Trans. Neural Syst. Rehabil. Eng.*, vol. 11, no. 2, pp. 141–144, Jun. 2003.

[43] M. R. N. Kousarrizi, A. A. Ghanbari, M. Teshnehlab, M. A. Shorehdeli, and A. Gharaviri, "Feature extraction and classification of EEG signals using wavelet transform, SVM and artificial neural networks for brain computer interfaces," in *Proc. Int. Joint Conf. Bioinf., Syst. Biol. Intell. Comput.*, 2009, pp. 352–355.

[44] B. V. Dasarathy, *Nearest Neighbor (NN) Norms: NN Pattern Classification Techniques*. IEEE Computer Society Press, 1991.

[45] M. Manjusha and R. Harikumar, "Performance analysis of KNN classifier and K-means clustering for robust classification of epilepsy from EEG signals," in *Proc. Int. Conf. Wireless Commun., Signal Process. Netw. (WiSPNET)*, Mar. 2016, pp. 2412–2416.

[46] A. Bablani, D. R. Edla, and S. Dodia, "Classification of EEG data using K-nearest neighbor approach for concealed information test," *Proc. Comput. Sci.*, vol. 143, pp. 242–249, 2018.

[47] Z. Y. Ong, A. Saidatul, and V. Vikneswaran, "Comparison between predicted results and built-in classification results for brain–computer interface (BCI) system," in *Proc. AIP Conf.*, vol. 2339, 2021, Art. no. 020167.

[48] H. Wang and Y. Zhang, "Detection of motor imagery EEG signals employing naïve Bayes based learning process," *Measurement*, vol. 86, pp. 148–158, May 2016.

[49] T. N. Alotaiby, S. A. Alshebeili, T. Alshawi, I. Ahmad, and F. E. Abd El-Samie, "EEG seizure detection and prediction algorithms: A survey," *EURASIP J. Adv. Signal Process.*, vol. 2014, no. 1, p. 183, Dec. 2014.

[50] P. Tripathi, A. Kumar, R. Komaragiri, and M. Kumar, "A review on computational methods for denoising and detecting ECG signals to detect cardiovascular diseases," *Arch. Comput. Methods Eng.*, vol. 29, no. 1, pp. 1–40, Oct. 2021.

[51] W.-K. Tam, K.-Y. Tong, F. Meng, and S. Gao, "A minimal set of electrodes for motor imagery BCI to control an assistive device in chronic stroke subjects: A multi-session study," *IEEE Trans. Neural Syst. Rehabil. Eng.*, vol. 19, no. 6, pp. 617–627, Dec. 2011.

[52] H. H. Jasper, "The ten-twenty electrode system of the international federation," *Electroencephalogr. Clin. Neurophysiol.*, vol. 10, pp. 370–375, Jan. 1958.

[53] K. Belwafi, O. Romain, S. Gannouni, F. Ghaffari, R. Djemal, and B. Ouni, "An embedded implementation based on adaptive filter bank for brain–computer interface systems," *J. Neurosci. Methods*, vol. 305, pp. 1–16, Jul. 2018.

[54] R. Zhang, Q. Zong, L. Dou, and X. Zhao, "A novel hybrid deep learning scheme for four-class motor imagery classification," *J. Neural Eng.*, vol. 16, no. 6, Oct. 2019, Art. no. 066004.

[55] G. Dai, J. Zhou, J. Huang, and N. Wang, "HS-CNN: A CNN with hybrid convolution scale for EEG motor imagery classification," *J. Neural Eng.*, vol. 17, no. 1, Jan. 2020, Art. no. 016025.

[56] J. Jin, C. Liu, I. Daly, Y. Miao, S. Li, X. Wang, and A. Cichocki, "Bispectrum-based channel selection for motor imagery based brain–computer interfacing," *IEEE Trans. Neural Syst. Rehabil. Eng.*, vol. 28, no. 10, pp. 2153–2163, Oct. 2020.

[57] M. Rashid, B. S. Bari, M. J. Hasan, M. A. M. Razman, R. M. Musa, A. F. A. Nasir, and A. P. P. A. Majeed, "The classification of motor imagery response: An accuracy enhancement through the ensemble of random subspace K-NN," *PeerJ Comput. Sci.*, vol. 7, p. e374, Mar. 2021.

[58] M. I. Chacon-Murguia, B. E. Olivas-Padilla, and J. Ramirez-Quintana, "A new approach for multiclass motor imagery recognition using pattern image features generated from common spatial patterns," *Signal, Image Video Process.*, vol. 14, no. 5, pp. 915–923, Jul. 2020.

[59] M. T. Sadiq, X. Yu, Z. Yuan, and M. Z. Aziz, "Motor imagery BCI classification based on novel two-dimensional modelling in empirical wavelet transform," *Electron. Lett.*, vol. 56, no. 25, pp. 1367–1369, Dec. 2020.

[60] S. Sakhavi, C. Guan, and S. Yan, "Learning temporal information for brain–computer interface using convolutional neural networks," *IEEE Trans. Neural Netw. Learn. Syst.*, vol. 29, no. 11, pp. 5619–5629, Nov. 2018.

[61] P. Lu, N. Gao, Z. Lu, J. Yang, O. Bai, and Q. Li, "Combined CNN and LSTM for motor imagery classification," in *Proc. 12th Int. Congr. Image Signal Process., Biomed. Eng. Informat. (CISP-BMEI)*, 2019s, pp. 1–6.

[62] W. Qiao and X. Bi, "Deep spatial–temporal neural network for classification of EEG-based motor imagery," in *Proc. Int. Conf. Artif. Intell. Comput. Sci.*, Jul. 2019, pp. 265–272.

[63] M. Riyad, M. Khalil, and A. Adib, "MI-EEGNET: A novel convolutional neural network for motor imagery classification," *J. Neurosci. Methods*, vol. 353, Apr. 2021, Art. no. 109037.

[64] J. J. Liao, J. J. Luo, T. Yang, R. Q. Y. So, and M. C. H. Chua, "Effects of local and global spatial patterns in EEG motor-imagery classification using convolutional neural network," *Brain-Comput. Interfaces*, vol. 7, nos. 3–4, pp. 47–56, Oct. 2020.

[65] S. Xu, L. Zhu, W. Kong, Y. Peng, H. Hu, and J. Cao, "A novel classification method for eeg-based motor imagery with narrow band spatial filters and deep convolutional neural network," *Cognit. Neurodynamics*, vol. 16, pp. 379–389, Sep. 2022.